Molecular Biology Reports (2024) 51:184
https://doi.org/10.1007/s11033-024-09231-z

ORIGINAL ARTICLE

Heterologous expression and fibrillary characterization of the microtubule-binding domain of tau associated with tauopathies

Chong Peng[3] · Wei Wei[3] · Huitu Zhang[1,2,3] · Ying Wang[3] · Baogen Chang[3] · Wenping Zhao[3] · Longgang Jia[3] · Li Li[4] · Fuping Lu[1,2,3] · Fufeng Liu[1,2,3]

Received: 10 July 2023 / Accepted: 8 January 2024

Abstract

Background Neurofibrillary tangles (NFTs) are one of the most common pathological characteristics of Alzheimer's disease. The NFTs are mainly composed of hyperphosphorylated microtubule-associated tau. Thus, recombinant tau is urgently required for the study of its fibrillogenesis and its associated cytotoxicity.

Methods and results Heterologous expression, purification, and fibrillation of the microtubule-binding domain (MBD) of tau (tauMBD) were performed. The tauMBD was heterologously expressed in *E. coli*. Ni-chelating affinity chromatography was then performed to purify the target protein. Thereafter, tauMBD was systematically identified using the SDS-PAGE, western blot and MALDI-TOF MS methods. The aggregation propensity of the tauMBD was explored by both the thioflavin T fluorescence and atomic force microscopy experiments.

Conclusions The final yield of the recombinant tauMBD was ~20 mg L^{-1}. It is shown that TauMBD, in the absence of an inducer, self-assembled into the typical fibrils at a faster rate than wild-type tau. Finally, the in vitro cytotoxicity of tauMBD aggregates was validated using PC12 cells. The heterologously expressed tau in this study can be further used in the investigation of the biophysical and cellular cytotoxic properties of tau.

Chong Peng and Wei Wei have contributed equally to this work.

✉ Fuping Lu
lfp@tust.edu.cn

✉ Fufeng Liu
fufengliu@tust.edu.cn

[1] Key Laboratory of Industrial Fermentation Microbiology, Ministry of Education, Tianjin 300457, P. R. China

[2] Tianjin Key Laboratory of Industrial Microbiology, Tianjin 300457, P. R. China

[3] College of Biotechnology, Tianjin University of Science & Technology, Tianjin 300457, P. R. China

[4] College of Marine and Environmental Sciences, Tianjin University of Science & Technology, Tianjin 300457, P. R. China

Published online: 23 January 2024

Graphical abstract

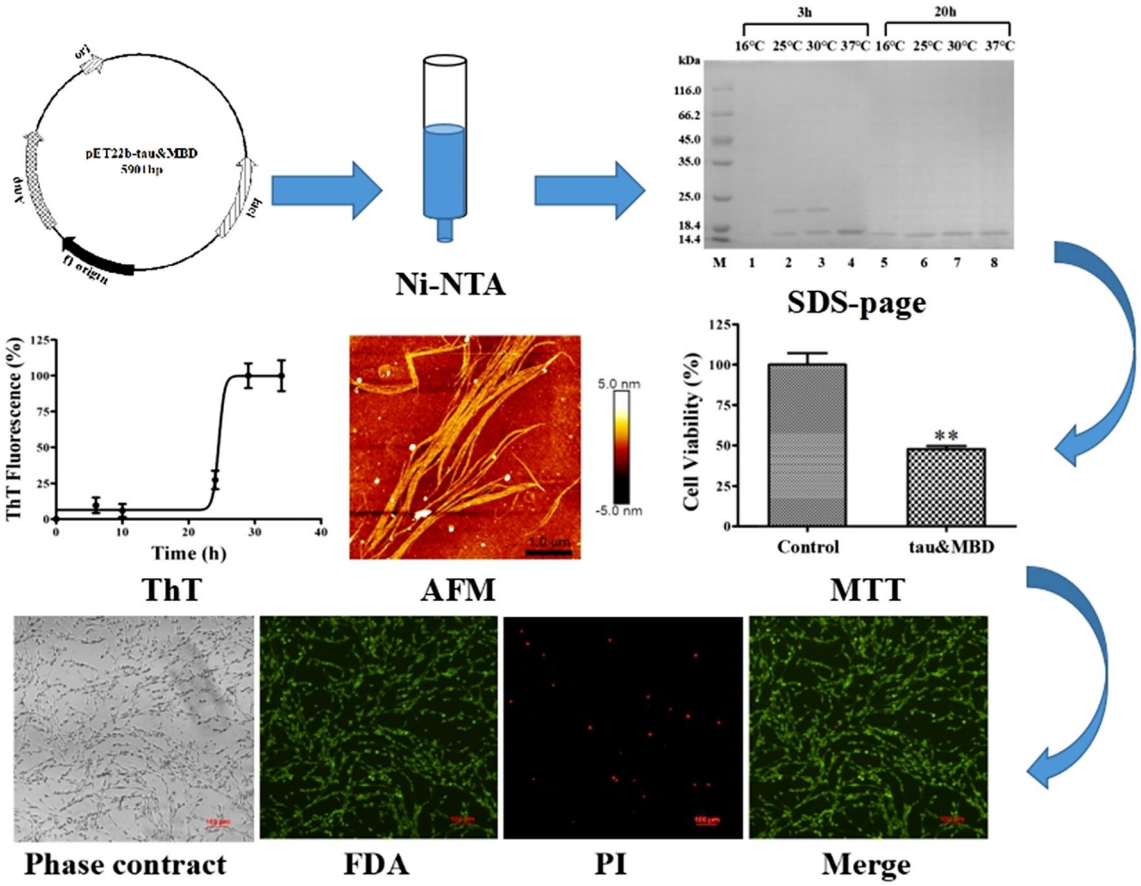

Keywords Alzheimer's disease · The microtubule-binding domain of tau · Heterologous expression · Fibrillogenesis

Introduction

Misfolding and the subsequent aggregation of tau can lead to a variety of tauopathies such as Alzheimer's disease (AD), chronic traumatic encephalopathy, Pick's disease, globular glial tauopathy, and corticobasal degeneration [1–4]. Among them, AD is a universal neurodegenerative disease with the feature of progressive dementia. Its main clinical manifestations are progressive cortical dysfunction, intellectual and cognitive impairment [5–7].

Tau, a microtubule-binding protein, is widely distributed in the nervous system. It plays a physiological function in stabilizing microtubules and regulating axonal transport [8, 9]. The full-length tau is composed of four regions: N-terminal projection domain (N), proline-rich domain (PRD), microtubule-binding domain (MBD) that contain four repeats (R), and C-terminal domain (Fig. 1). Tau binds to microtubule through the region of R1-R4. According to the number of N and R in MBD, six tau isoforms including 0N3R, 0N4R, 1N3R, 1N4R, 2N3R and 2N4R were identified [10]. The detailed information including major regions, location and the number of residues is shown in Fig. 1. Tree subtypes of 0N4R, 1N4R and 2N4R contain four repeat domains [1]. Previous studies have shown that the expression of these tau protein subtypes has a certain relationship with age [10]. For example, 0N3R only exists in the infant brain and the levels of 3R and 4R are consistent in the adult brain. In addition, the expression ratios of tau protein subtypes are different in different brain structures. Even in a single neuron, the positioning of various tau protein subtypes is also different. Many phenomena indicate that each tau protein subtype may play a different role [8, 11].

Plenty of tau proteins is needed in the research of tau aggregation and the development of tau aggregation inhibitor. However, because of the large molecular weight of tau, it is difficult to synthesize them using the solid-phase peptide synthesis technology. Microbial heterologous expression technology was used frequently to obtain macromolecular

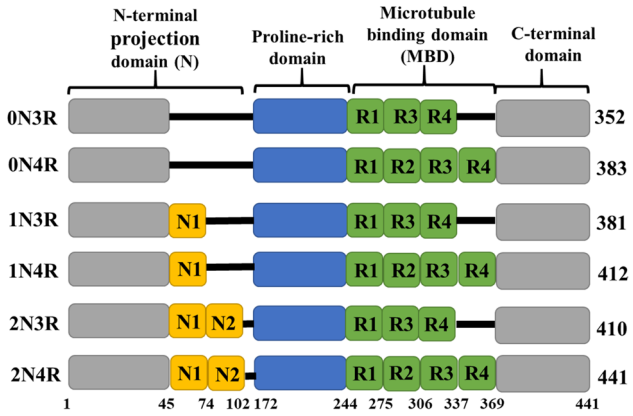

Fig. 1 Comparison of six isoforms including 0N3R, 0N4R, 1N3R, 1N4R, 2N3R, and 2N4R of human tau protein. The microtubule-binding domain (MBD) contains three or four repeats (R1, R2, R3 and R4). Repeats 1–4 are the core of the filaments

proteins containing more than 100 residues [12]. Prokaryotic and eukaryotic expression systems are commonly used to obtain recombinant tau proteins and their various isoforms [13–16]. For example, Karikari [13] used c-Myc fusion tag fusion to expressed the MBD of tau in *E. coil* (NEB-5a). The protein obtained by the method has good fibrosis ability and can be used for the research of aggregation characteristics and toxicity in vitro. Mo [14] expressed and purified the recombinant $tau_{244–372}$ fragment and its mutants in *E. coli*, and investigated the effect of zinc on its aggregation. Similarly, Zhu [16] heterologously expressed $tau_{244–372}$ fragment in *E. coli* and characterized the interactions between this recombinant tau fragment and heparin-induced fibril formation. In addition to *E. coli* expression system, Vandebroek [15] attempted to use yeast expression system to obtain the MBD domain of tau. The yeast expression system was used to express tau and its post-modified ones. Moreover, the obtained tau protein also exhibits excellent fibrillogenesis characteristics and induces the strong cytotoxicity. It implies that the recombinant tau protein can be applied in biochemical research and the screening of tau protein aggregation inhibitors.

In this study, the optimal conditions for heterologous expression and isolation of tauMBD in *E. coli* were identified. The plasmid pET22b was used to construct the recombinant vector. The MBD of tau (tauMBD) was highly expressed in *E. coli*. Ni-chelating affinity (Ni-NTA) chromatography was then performed to purify the recombinant protein. The purified tauMBD was identified by SDS-PAGE, western blot, and MALDI-TOF-MS. Finally, the aggregation characteristics and cytotoxicity of the aggregates were verified by several biophysical methods, such as thioflavin T fluorescent staining experiment, atomic force microscope (AFM) experiment, and cytotoxicity assays.

Materials and methods

Materials

The plasmid pET22b, the *E. coli* JM109, *E. coli* BL21 (DE3) strains and the PC12 cell line were stored in our laboratory. The restriction endonucleases *Nde* I, *Xho* I and T4 DNA ligase were acquired from Takara (Dalian, China). The codon optimized tauMBD gene was obtained from GENEWIZ Corporation (Suzhou, China). The sequence analysis of tauMBD gene was also performed by GENEWIZ. Primers were synthesized by BGI (Shenzhen, China). The mouse anti-His_6 antibody, goat anti-mouse IgG and BeyoECL Star Kit was purchased from Beyotime Biotechnology Corporation (Shang Hai, China).

Heterologous expression of recombinant tauMBD protein

The full-length cDNA of tauMBD fragment was codon-optimized according to *E. coli* codon usage preference and then was synthesized by GENEWIZ Company (Suzhou, China) in the form of pUC57-tauMBD plasmid. The His_6 tag's gene was added at the end of tauMBD's gene to facilitate protein purification. After double digestion by *Nde* I and *Xho* I, the tauMBD was gel purified. The target gene was then cloned into the same restriction enzyme cutting sites of plasmid pET22b to yield pET22b-tauMBD. The obtained recombinant plasmid pET22b-tauMBD was amplified in *E. coli* JM109. Three positive single colonies were selected for colony PCR verification (primers *Nde* I-tauMBD-F: GGAATTCCATATGCAGACCGCCCCGGTTCCGAT and *Xho* I-tauMBD-R: CCGCTCGAGTTAATGATGGTG ATGATGGT) and the plasmids from single colonies were extracted for double digestion. The right recombinant plasmid was thereafter transformed into *E. coli* BL21 (DE3) competent cells for inducible expression under a T7 promoter. Signal colonies were inoculated in 5 mL LB containing 100 μg mL^{-1} ampicillin and cultured overnight. Then signal colonies containing the correct recombinant plasmid were inoculated to 200 mL LB media with the same antibiotic and cultured to an OD600 of 0.6–0.8. Eight groups of cells were induced with 0.5 mM isopropyl-β-D-thiogalactoside (IPTG) at 16 °C, 25 °C, 30 and 37 °C for 3 and 20 h.

Purification of the recombinant tauMBD protein

The *E. coli* bacteria were harvested by centrifugation and then were suspended in lysis buffer (20 mM Tris, 500 mM NaCl, 1 mM dithiothreitol, 20 mM imidazole, pH 7.4).

10 μM phenylmethylsulfonyl fluoride (PMSF) was then added to the buffer. The cells were then crashed by sonication with the Sonifier Scientz-950E (Ning Bo Scientz Biotechnology Company, China). And the cell fragmentation fluid was centrifuged at 12,000×*g* for 30 min, collected the supernatant and pellet. The supernatant was mixed with Ni-NTA resin to bind the target protein to the resin after filtering with a 0.22 μm filter. And then the resin was washed with wash buffer (20 mM Tris, 500 mM NaCl, 50 mM imidazole, 1 mM dithiothreitol, pH 7.4) to get out the other proteins that are loosely bound. Finally, the tauMBD was eluted by elution buffer (20 mM Tris, 500 mM NaCl, 500 mM imidazole, 1 mM dithiothreitol, pH 7.4). The purified proteins were dialyzed by 3.0 kDa dialysis bag using ultra-pure water for the removal of imidazole, NaCl and other components, then were treated by freeze-drying and stored at − 20 °C for reserve.

SDS-PAGE analysis

Prepare 20 μL protein sample and add 5 μL SDS-PAGE loading buffer (contain 10% β-mercaptoethanol). The mixture was denatured at 100 °C for 10 min. 15 μL of the denatured protein samples were then analyzed by SDS-PAGE on a 12% running gel to determine the size and purity of the sample. The gel was dyed with Coomassie brilliant blue R250 solution.

Western blot analysis

The purified protein was for the SDS-PAGE and the protein traces on the gel was transferred to the polyvinylidene fluoride (PVDF). The standard wet film transfer device (Bio-Rad, USA) was used to set the membrane current of 100 V and the transfer time was 30–60 min [17]. The PVDF was sealed in 5% skimmed milk powder solution for 60 min. After that, TBS-T (20 mM Tris-HCl, 150 mM NaCl, 0.05% (V/V) Tween 20, pH 7.4) was used to wash the PVDF for 3 times. The blocked PVDF was then put in the mouse anti-His_6 antibody and incubated overnight at 4 °C [18]. After washed with TBS-T buffer for another 3 times, the PVDF was thereafter incubated with goat anti-mouse antibody for 2–3 h at normal temperature. Then the PVDF was cleaned with TBS-T buffer for 3 times and treated by BeyoECL Star Kit. Chemiluminescence imager (Clinx Science Instruments, Shang Hai, China) was used to observe the protein traces. The dilution multiples of antibodies were 1:1000. The first antibody was diluted with 5% skimmed milk powder solution and the second antibody IgG was diluted with TBS-T buffer solution.

MALDI-TOF MS analysis

Two milligrams of tauMBD was dissolved in 10 mL TA30 solvent (30% acetonitrile-0.1% trifluoroacetic acid), the protein solution concentration is 2 mg mL^{-1}. Then, dilute the protein solution tenfold, and 2 μL of protein solution (contains 4 μg of protein) was mixed with 2 μL HCCA matrix (a saturated solution of α-Cyano-4-hydroxycinnamic acid in TA30). Thereafter, 2 μL of the mixture was added on the MTP 384 target ground steel T F (Bruker, USA). After the sample is naturally dried, it is detected by MALDI-TOF ultrafleXtreme (Bruker, USA).

Thioflavin T fluorescence assay

The aggregation characteristics of tauMBD protein were detected by ThT fluorescence staining experiment. The detail ThT experimental procedures was provided in our previous studies [19, 20]. The in situ culture method was adopted with little modification: the purified tauMBD was firstly dissolved in PBS buffer (pH 7.4) to the concentration of 100 μM. The ThT stock solution was also prepared with PBS buffer at a concentration of 250 μM. For fluorescence assay, 50 μL tauMBD solution, 60 μL ThT stock solution, and 90 μL PBS buffer was added to the 96-well plates and incubated at 250 rpm and 37 °C. The fluorescence (the excitation wavelength is 440 nm, the emission wavelength is 480 nm) was detected at different time periods. Three repeated ThT experiments were performed.

Atomic force microscopy experiment

The detailed AFM methods were described in our previous studies [21, 22]. The morphologies of the final samples in ThT fluorescence experiments were observed using AFM. In brief, 20 μL of target protein solution was placed to the fresh mica sheet, then incubated at room temperature for 10 min, and let stand for 10–20 min for absorption. The mica sheet was then cleaned by water to wipe off particle salt and unabsorbed protein [23]. And let the excess water dry naturally. AFM Multimode 8 (Bruker, USA) was used to implement the intelligent mode AFM imaging in air with a standard Scan Asyst-Air silicon probe tip. The important parameter settings and the obtained AFM images processing refer to our previous research [20].

Cytotoxicity assay

The experimental procedure of PC12 cell culture is descripted in our previous studies [20, 24, 25]. First, the cells were inoculated in 96-well plates with 90 μL medium to a density of ~ 5×10^4 cells per well and incubated at 37 °C for 24 h. 10 μL of tauMBD that pre-incubated for 5d were

added into the cells and incubated for another 48 h. Then, 10 µL of MTT solution (5.0 mg mL^{-1}) was added to the culture medium of PC12 cells and cultured for 4 h. Then the medium was removed. The cells were lysed in 100 µL DMSO at 37 °C. Then the absorbance was detected by the microplate reader (Infinite 200 PRO Laboratories, TECAN, Austria), the determine wavelength was 570 nm.

In order to further study the toxicity of tauMBD to PC12 cell lines, the fluorescein diacetate/propidium iodide (FDA/PI) mixed double staining method were also performed to distinguish live and dead cells [26]. The cells were seeded into 6-well plates with 2 mL fresh medium to a density of ~ 5×10^4 cells per well. After 24 h, the pre-incubated protein was added to the 6-well plates. The PC12 cells were cultured together with the tauMBD fibrils for another 48 h. Then the medium was removed. The cells were mixed into working solutions containing 10 µg mL^{-1} FDA and 5 µg mL^{-1} PI. After 15 min, the PC12 cells were washed with PBS. BX53 fluorescence microscope (Olympus, Japan) was used to observe the cells.

Results

Heterologous expression, purification, and identification of the recombinant tauMBD

According to the amino acid sequence of tauMBD and the codon usage preference of *E. coli*, a codon-optimized cDNA was synthesized. The cDNA was inserted into the expression vector of pET22b to yield the vector of pET22b-tauMBD, in which the expression the tauMBD gene was controlled by the T7 promoter, the lac operator gene, and the RBS site. To facilitate protein purification, a His_6 tag was fused to the C-terminus of the recombinant tauMBD. The whole framework of the expression vector and the detailed sequence of the synthesized tauMBD gene were shown in Fig. 2a. The recombinant plasmid was preliminarily verified by individual bacterial colonies PCR (Fig. 2b) and double digestion verification (Fig. 2c), as well as the gene sequencing analysis further proved that the recombinant plasmid was successfully constructed. The recombinant expression vector was introduced into the expression host *E. coli* BL21 (DE3), and the individual bacterial colonies PCR (Fig. 2d) showed that the recombinant plasmid was successfully transferred into *E. coli* BL21 (DE3). The theoretical molecular weight of recombinant tauMBD including His_6 tag obtained by heterologous expression is 14.6 kDa. SDS-PAGE assay of the cell fragmentized liquid revealed a distinctly protein bond of 14.6 kDa (Fig. 3a), the tauMBD band in the red box), which is similar to the predicted mass of the tauMBD with an additional His_6 tag. It was proved that the recombinant protein was expressed in a soluble form. The one-step Ni-NTA chromatography purification process of the sample (Fig. 3b), the tauMBD bands in the red box), and the purity of the protein eluted (Fig. 3b, lane 5) was 95%. Therefore, it is possible to express tau MBD correctly and purify it successfully.

As His_6 tag is linked to its C-terminal of the tauMBD, western blot analysis was also conducted with His_6 tag antibody. A clear print of recombinant tauMBD protein is shown in Fig. 3c. It once again demonstrated that the tauMBD-His_6 was correctly expressed. Then, the recombinant protein was further validated by identifying its molecular weight by MALDI TOF mass spectrometry. Figure 3d shows the result. In the range of m/z 10,000–20,000, the productions acquired from the break of charged ions at m/z 14,633 correspond to the recombinant tauMBD polypeptide with a theoretical molecular weight of 14,633 Da. Based on the above analysis, we confirmed that tauMBD was successfully purified.

Optimization of expression conditions of recombinant tauMBD protein

To increase the expression level of the recombinant tauMBD in a soluble state, the expression conditions including induction temperature and induction time were optimized, as shown in Fig. 4a. For convenient comparison, the histogram of tauMBD bands in Fig. 4b was calculated by gray level analysis in image J software. The histogram intuitively showed that the yield of tauMBD increases gradually with the increase of temperature whether it is induced for 3 or 20 h. On the contrary, the yield of tauMBD did not increase after 20 h of induction, and the yield of tauMBD decreased even compared with that after 3 h of induction. For example, the yields after 3 h of induction at both 30 and 37 °C were significantly higher than that after 20 h of induction. Proved that prolonged induction time did not increase the soluble expression of tauMBD. They indicated that the highest expression level of tauMBD was obtained under such conditions: adding IPTG to a final concentration of 0.5 mM when the growth density of recombinant strain (OD_{600}) reached 0.6–0.8, inducing 3 h at a temperature of 37 °C. Under these conditions, the protein was expressed in large quantities. However, it is worth noting the presence of a secondary band above the monomer in Fig. 4a, suggesting the possible existence of dimers or larger oligomers. While our findings confirm that a 3-h induction at 37 °C leads to the optimal expression of tauMBD, it is imperative to take into account the potential formation of such higher-order assemblies and the effects this may exert on purification strategies. Conversely, incubation at all temperatures for 20 h yields monomers of exceptional purity. Therefore, it is essential to emphasize the importance of careful temperature control during the induction process

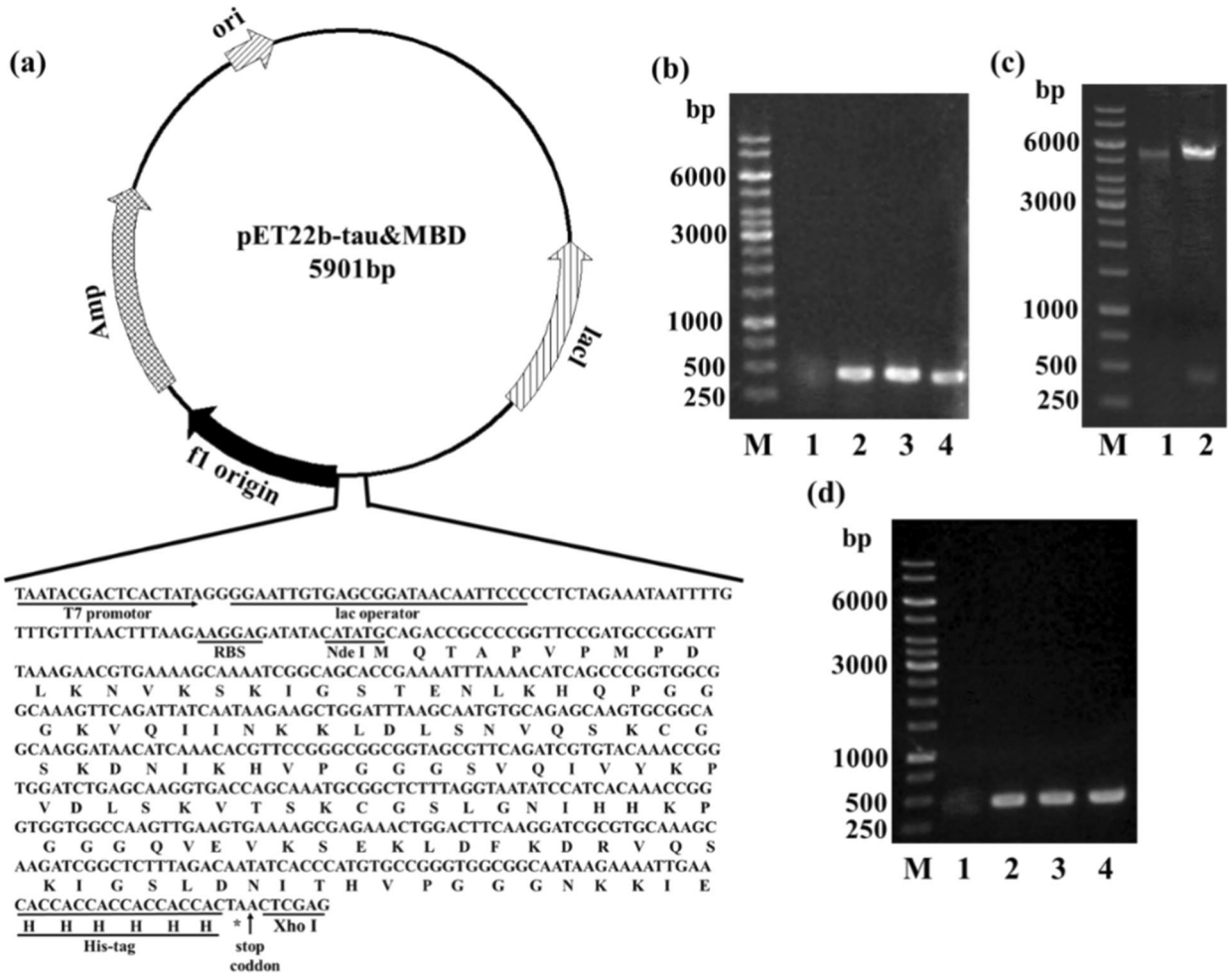

Fig. 2 Construction of pET22b-tauMBD expression vector and recombinant BL21-pET22b-tauMBD strain. **a** Schematic diagram of the expression vector pET22b-tauMBD. TauMBD sequence was inserted into the Nde I and Xho I sites of pET22b. **b** Individual bacterial colonies PCR of JM109-pET22b-tauMBD strain. M: 1 kb ladder; lane 1: transformant of JM109-pET22b strain; lanes 2–4: three transformants of JM109-pET22b-tauMBD strain. **c** Double digestion validation of recombinant plasmid pET22b-tauMBD with Nde I and Xho I. M: 1 kb ladder; 1: pET22b vector; 2: pET22b-tauMBD recombinant expression vector. **d** Individual bacterial colonies PCR of BL21-pET22b-tauMBD strain. M: 1 kb ladder; lane 1: transformant of BL21-pET22b; lanes 2–4: three transformants of BL21-pET22b-tauMBD

to minimize the formation of dimers or oligomers. The purified protein solution was freeze-dried and weighed. It was found that ~ 20 mg of protein was obtained per liter of fermentation broth.

After purification with Ni-NTA, the purity of recombinant tauMBD protein reached more than 95% and the yield of the purified protein reached ~ 20 mg L^{-1}, which is greatly higher than previous studies [13, 15, 27–30]. For example, Karikari [13] used c-Myc fusion tag fusion to expressed the MBD of tau in *E. coil* (NEB-5a). However, the yield of tau obtained in this study was not high enough, approximately 11 mg L^{-1}. In addition to *E. coli* expression system, Vandebroek [15] attempted to use yeast expression system to obtain the MBD domain of tau. However, the yield of tau was as low as 20 μg L^{-1}.

Aggregation properties characterization of recombinant tauMBD

Tau fibrillization was characterized using ThT fluorescence analysis method. As one of the gold standards for the quantitative determination of amyloid fibrils, the basic principle is that ThT molecules can stimulate fluorescence by binding to the β-sheet-rich tau aggregates, while free ThT does not fluoresce [31–33]. Therefore, the aggregation kinetics of amyloid proteins can be investigated by detecting the change of ThT fluorescence intensity. Figure 5a shows the aggregation kinetics curve of tauMBD detected by ThT fluorescence assay. As shown in Fig. 5a, after the lag phase about 24 h, the ThT signal of tauMBD increased dramatically in just 5 h, and reached the stable phase after

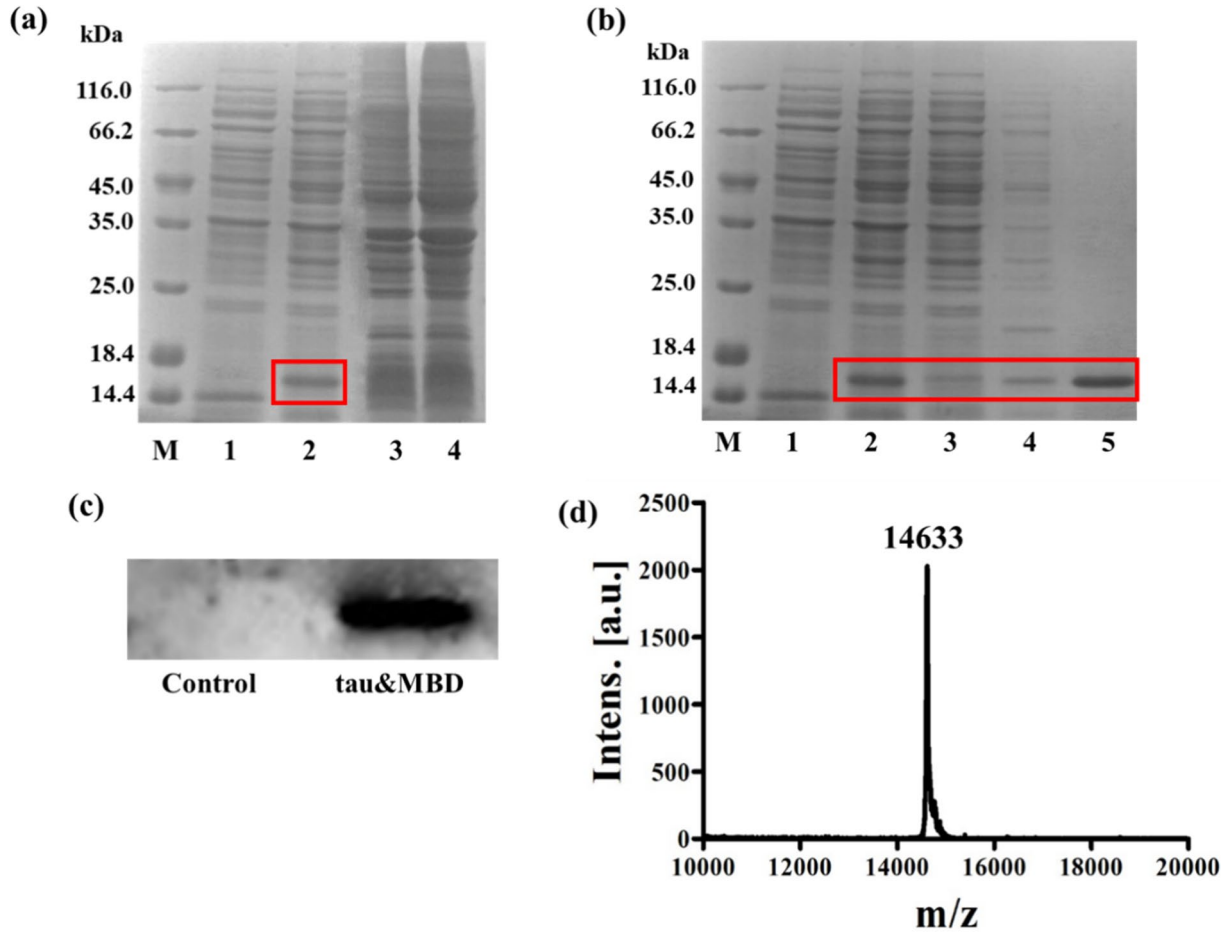

Fig. 3 Heterologous expression and purification of the recombinant tauMBD. **a** SDS-PAGE analysis of the supernatant and pellet obtained from BL21-pET22b-tauMBD strain after induced with 0.5 mM IPTG and lysis by sonication. M: protein marker; lane 1: supernatant of BL21-pET22b; lane 2: supernatant of BL21-pET22b-tauMBD, tauMBD is marked by a red box; lane 3: pellets of BL21-pET22b; lane 4: pellets of BL21-pET22b-tauMBD. **b** SDS-PAGE analysis of samples from different steps of purification with Ni-NTA. M: protein marker; lane 1: supernatant of BL21-pET22b; lane 2: BL21-pET22b-tauMBD; lane 3: flow-through of the soluble protein eluted from the Ni-NTA column; lane 4: the loosely bound protein eluted by the wash buffer; lane 5: relatively pure tauMBD eluted by the elution buffer. TauMBD is marked by a red box. **c** Western blot analysis of the recombinant tauMBD after purification. Control: supernatant of BL21-pET22b; tauMBD: relatively pure tauMBD eluted by the elution buffer. **d** MALDI-TOF-MS analysis of the recombinant tauMBD

about 30 h. The typical sigmoidal curve of tau fibrillogenesis indicates that the protein is gradually assembled from monomers into aggregates with β-sheet-rich structure. It is worth noting that tau is natively unfolded, contains a high concentration of positively and negatively charged residues, and is highly soluble in solution, thus resisting spontaneous aggregation [8]. Biochemical "inducers" of tau aggregation are extensively utilized to trigger and accelerate the aggregation of tau in vitro. Heparin, a frequently used inducer of tau aggregation, prompts the formation of polymorphic tau aggregate structures that differ from those observed in filaments isolated from diseases [34]. In the current study, tauMBD was observed to aggregate at a relatively rapid pace in the absence of an inducer, rendering it a promising molecular entity for investigating tau aggregation and identifying inhibitors of tau fibrillization.

The final samples of ThT fluorescence experiments were analyzed using AFM. As shown in Fig. 5b, after incubation, AFM images certified that tauMBD aggregated into typical, long branched fibrils. Figure 5c is the height image of the mature fibril cross section. The scale bar indicated that the fibrils had a height of about 1–3 nm. Compared to other amyloid proteins such as β-amyloid and α-synuclein, the fibrils of tau were thinner, which is similar to fibril obtained from previous studies [35].

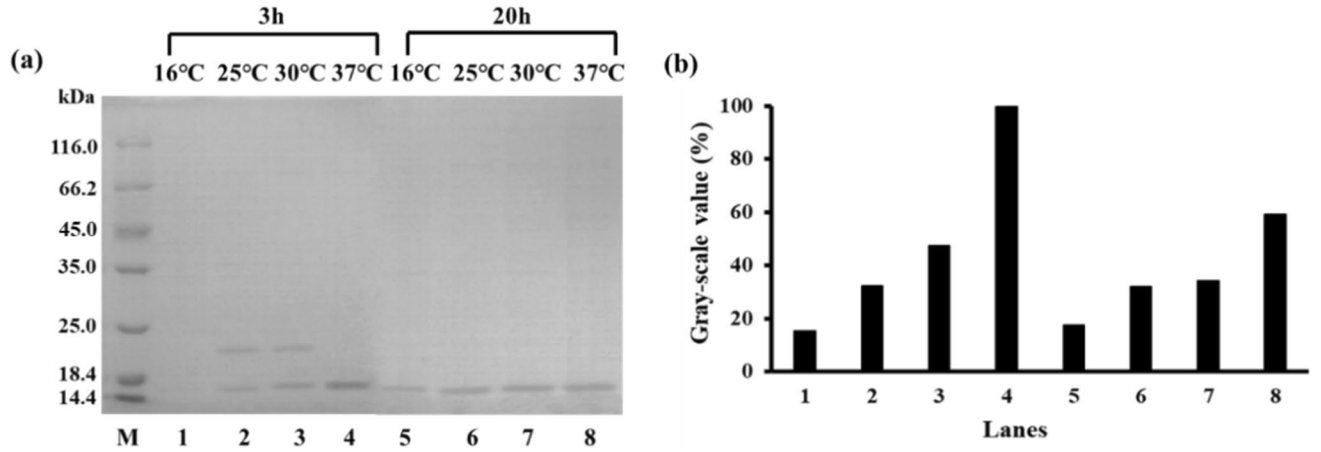

Fig. 4 Optimization of expression conditions of recombinant tauMBD. SDS-PAGE analysis was performed after the protein was purified. **a** Protein expression after 3 and 20 h of induction at four different temperatures. M: protein molecular weight marker; lanes 1–4: Protein expression after 3 h of induction at 16 °C, 25 °C, 30 and 37 °C; lanes 5–8: Protein expression after 20 h of induction at 16 °C, 25 °C, 30 and 37 °C; **b** Image J was used to analyze the gray value of tauMBD bands in (**a**)

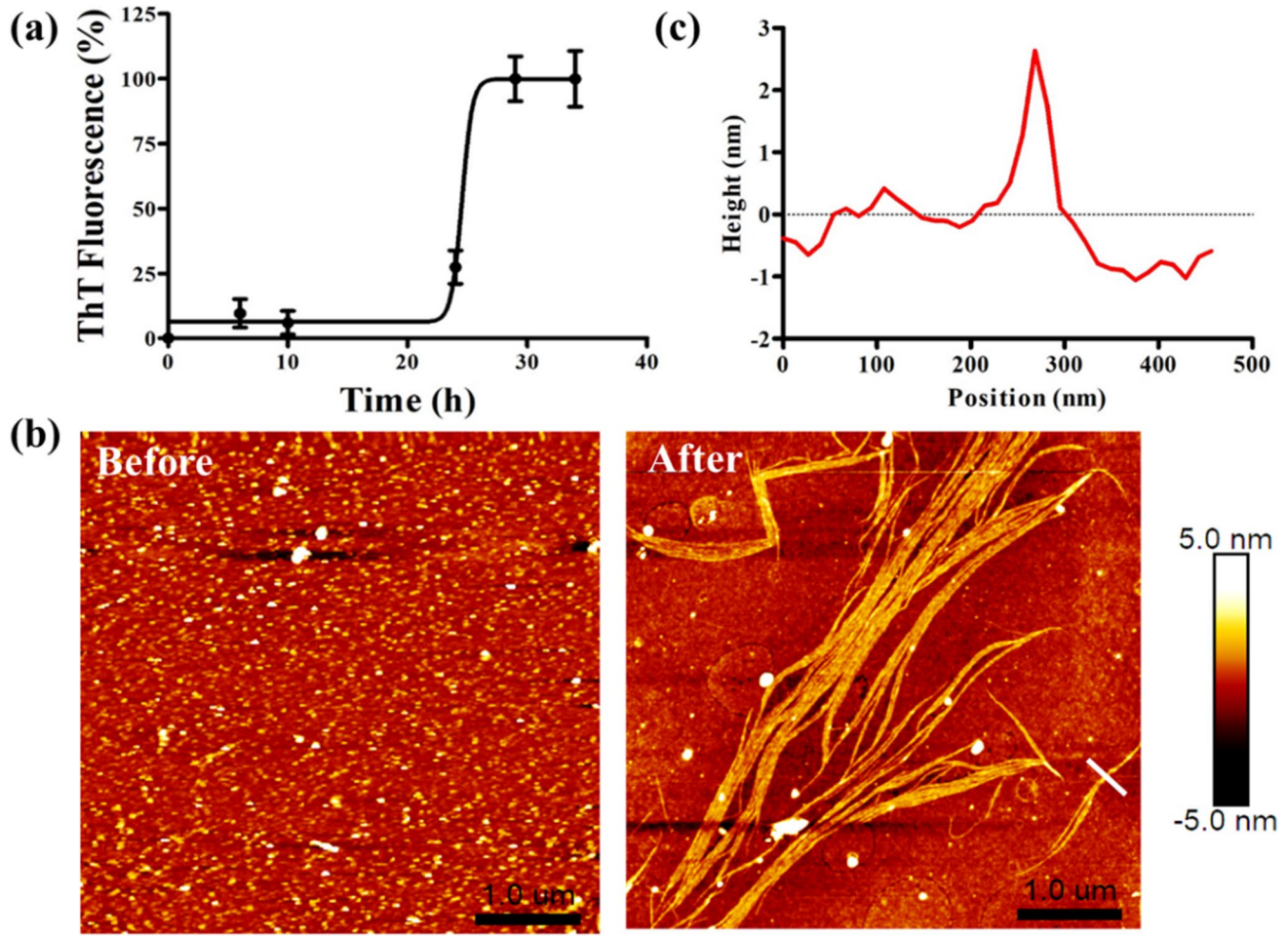

Fig. 5 Aggregation properties characterization of recombinant tauMBD. **a** Aggregation kinetics curve of recombinant tauMBD was monitored by ThT fluorescence. **b** Morphology of aggregates formed by the recombinant tauMBD. Before: AFM images of recombinant tauMBD before incubation; After: AFM images of recombinant tauMBD after incubation for 5 d at 37 °C. **c** Height of the cross sections drawn over the fibrils after incubation

Cytotoxicity of the recombinant tauMBD

PC12 cells line is widely used in the field of neuropharmacology and cytotoxicity because that it has versatility in pharmacological operation, convenience in cultivation, and detailed knowledge on proliferation and differentiation [20, 36]. We cultured PC12 cells together with tauMBD fibrils for another 48 h. Then we used MTT assay to detect cell viability. The control group's cell viability was assigned as 100%. Figure 6a shows that the viability of the cells co-incubated with tauMBD fibrils was about 47.7%, which undoubtedly proved the strong cytotoxicity of tauMBD fibrils. To further analyze the toxicity of the aggregated tauMBD fibrils on PC12 cells, living and dead cells were labeled by FDA/PI mixed double staining. Figure 6b reveals that compared with the control group, the total number of living cells co-cultured with tauMBD fibrils was reduced. There were almost no dead cells with PI-marked in the control group. In the cells treated with tauMBD fibrils, the number of PI-positive red labels was obviously more than that in the control group. The above two cytotoxicity experiments show that the fibrils formed by the recombinant tau has a strong cytotoxicity to PC12 cells.

Recent studies have suggested that in addition to fibrils, oligomers may be present following tau aggregation [37]. These oligomers have been proposed to be the more toxic species [38–41]. The presence of both oligomers and fibrils in tau aggregation raises intriguing questions about their individual contributions to cytotoxicity. While our study focused on the evaluation of tauMBD fibrils, it is crucial to acknowledge the potential role of oligomers in the observed cytotoxicity. In our experiment, we did not

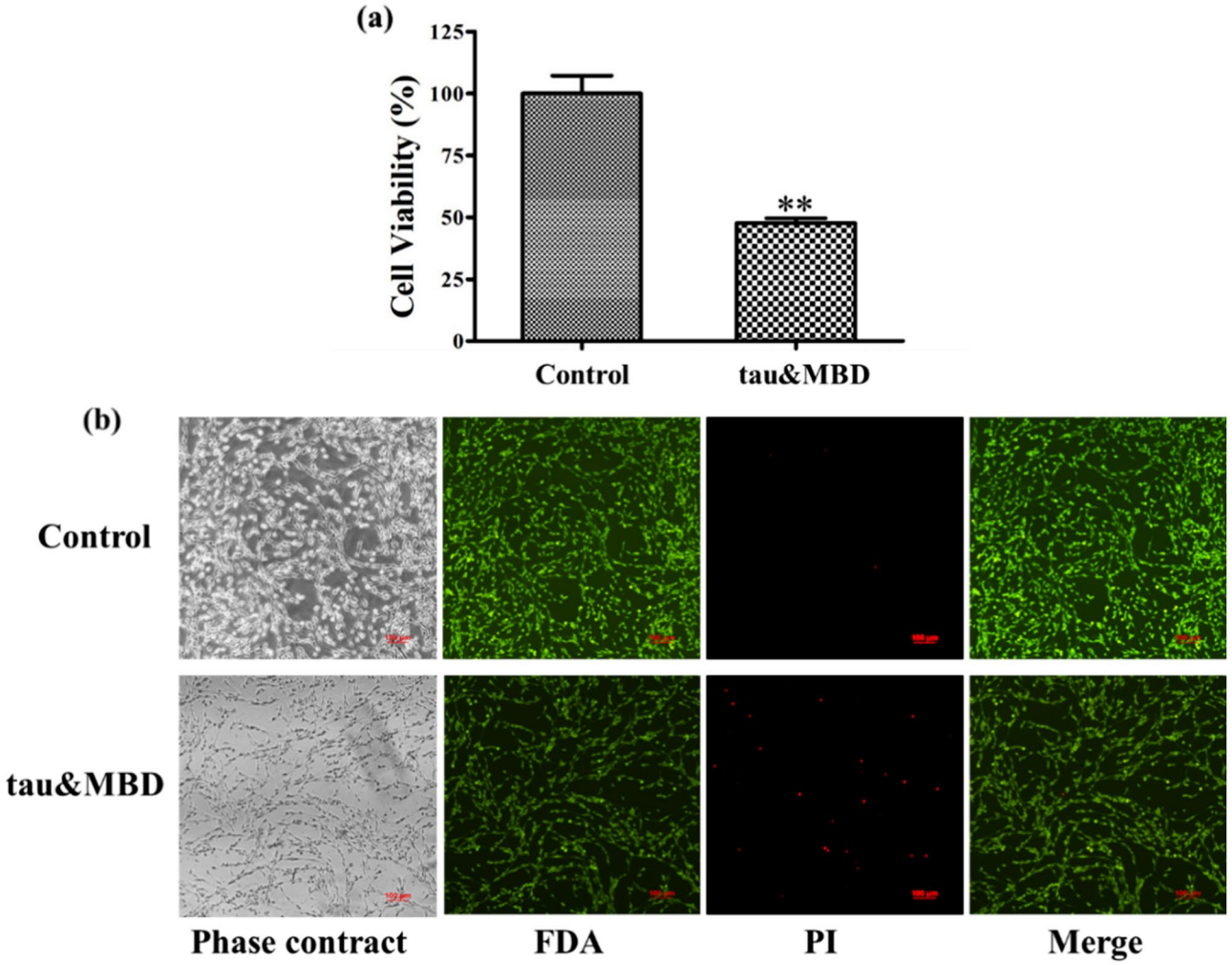

Fig. 6 Cytotoxicity of recombinant tauMBD aggregates toward PC12 cells. **a** PC12 cells were treated with or without tauMBD for 48 h and then MTT assay was performed. Values are relative to those of control cells mock-treated with complete medium alone. Values represent the means ± SD ($n = 3$). **$p < 0.05$, compared to the control. **b** The cell death induced by recombination tauMBD aggregation as probed by FDA/PI double staining of PC12 cells

directly detect the presence of oligomers, which is a matter that requires further investigation. Future studies could explore the ratio of oligomers to fibrils in tauMBD fibers, as well as their specific effects on PC12 cells.

In conclusion, our findings support the strong cytotoxicity of tauMBD fibrils on PC12 cells, indicating that the recombinant protein has good biological activity and can be applied to all aspects of tau protein research. Further research is needed to fully understand the mechanisms behind tau-induced cytotoxicity and to develop strategies to mitigate the toxic effects of these aggregated species in neurodegenerative disorders.

Discussion

In this research, we carried out a one-step method for the heterologous expression and purification of recombinant tauMBD. The recombinant tauMBD with a yield of ~ 20 mg L^{-1} was obtained by optimizing induced expression conditions and Ni-NTA purification. SDS-PAGE, western blot, and MALDI TOF-MS then were used to identify the recombinant tauMBD. ThT fluorescence assays and AFM experiment have illustrated the impressive aggregation activity of the tauMBD. The recombinant tauMBD displayed a faster rate of self-assembly into typical fibrils compared to wild-type tau, even in the absence of an inducer. These findings suggest that tauMBD may have a higher propensity for aggregation. Moreover, the in vitro cytotoxicity experiment verified that the recombinant tauMBD aggregates had a strong cytotoxic effect on PC12 cells, indicating its potential to cause cellular damage. The heterologously expressed tauMBD in this study can, therefore, serve as a valuable tool for investigating the biophysical and cellular cytotoxic properties of tau, which could ultimately lead to a better understanding of the underlying mechanisms of tauopathies.

Future research directions could include exploring the structural and molecular basis of tauMBD aggregation, investigating the role of tauMBD aggregates in neurodegenerative diseases, and evaluating potential therapeutic interventions targeting tauMBD aggregation. To sum up, this method enables the high yield of recombinant tauMBD, which can facilitate the study of the biochemical, physiological, and toxicity of tau and its isoforms. Beyond that, tau maintains the stability of the microtubules by binding to the microtubules through the MBD. It is an important core fragment of tau. It is more meaningful and persuasive to use this fragment to study the physiological, biochemical and aggregation characteristics of tau and to screen for various aggregation inhibitors.

Acknowledgements The authors would like to thank Wenqian Wang, Lei Zhao and Ailan Huang, for the invaluable assistance and inspiring discussions.

Funding This study was funded by the National Key Research and Development Program (2018YFA0901700), the National Natural Science Foundation of China (Nos. 21908165, 21878234, 21576199) and the Natural Science Foundation of Tianjin from the Tianjin Municipal Science and Technology Commission (Contract No. 18JCZDJC33000).

Data availability No Data associated in the manuscript.

Declarations

Conflict of interest We declare that there is no conflict of interest regarding the publication of this work.

Ethical approval This article does not contain any studies with human participants or animals performed by any of the authors.

References

1. Fitzpatrick AWP, Falcon B, He S, Murzin AG, Murshudov G, Garringer HJ, Crowther RA, Ghetti B, Goedert M, Scheres SHW (2017) Cryo-EM structures of tau filaments from Alzheimer's disease brain. Nature 547:185–190
2. Ghetti B, Oblak AL, Boeve BF, Johnson KA, Dickerson BC, Goedert M (2015) Frontotemporal dementia caused by microtubule-associated protein tau gene (MAPT) mutations: a chameleon for neuropathology and neuroimaging. Neuropath Appl Neuro 41:24–46
3. Goedert M (1993) Tau protein and the neurofibrillary pathology of Alzheimer's disease. Trends Neurosci 16(11):460–465
4. Grundke-Iqbal I, Iqbal K, Tung YC, Quinlan M, Wisniewski HM, Binder LI (1986) Abnormal phosphorylation of the microtubule-associated protein tau (tau) in Alzheimer cytoskeletal pathology. Proc Natl Acad Sci USA 83(13):4913–4917
5. Carter J, Anderton B (1994) Molecular pathology of Alzheimer's disease. Br J Hosp Med 51(10):522–528
6. Hardy JA, Higgins GA (1992) Alzheimer's disease: the amyloid cascade hypothesis. Science 256(5054):184–185
7. Yankner BA, Duffy LK, Kirschner DA (1990) Neurotrophic and neurotoxic effects of amyloid beta protein: reversal by tachykinin neuropeptides. Science 250(4978):279–282
8. Wang Y, Mandelkow E (2016) Tau in physiology and pathology. Nat Rev Neurosci 17:22–35
9. Rademakers R, Cruts M, van Broeckhoven C (2004) The role of tau (MAPT) in frontotemporal dementia and related tauopathies. Hum Mutat 24(4):277–295
10. Verwilst P, Kim HS, Kim S, Kang C, Kim JS (2018) Shedding light on tau protein aggregation: the progress in developing highly selective fluorophores. Chem Soc Rev 47:2249–2265
11. Arendt T, Stieler JT, Holzer M (2016) Tau and tauopathies. Brain Res Bull 126(3):238–292
12. Jia LG, Zhao WP, Wei W, Guo X, Wang WJ, Wang Y, Sang JC, Lu FP, Liu FF (2020) Expression and purification of amyloid β-protein, tau, and α-synuclein in *Escherichia coli*: a review. Crit Rev Biotechnol 40(4):475–489
13. Karikari TK, Turner A, Stass R, Lee LCY, Wilson B, Nagel DA, Hill EJ, Moffat KG (2017) Expression and purification of tau protein and its frontotemporal dementia variants using a cleavable histidine tag. Pro Expres Purif 130:44–54

14. Mo ZY, Zhu YZ, Zhu HL, Fan JB, Chen J (2009) Low micromolar zinc accelerates the fibrillization of human tau via bridging of Cys-291 and Cys-322. J Biol Chem 284:34648–34657
15. Vandebroek T, Vanhelmont T, Terwel D, Borghgraef P, Lemaire K, Snauwaert J, Wera S, Leuven FV, Winderickx J (2005) Identification and isolation of a hyperphosphorylated, conformationally changed intermediate of human protein tau expressed in yeast. Biochemistry 44(34):11466–11475
16. Zhu HL, Fernandez C, Fan JB, Shewmaker F, Chen J, Minton AP, Liang Y (2010) Quantitative characterization of heparin binding to tau protein implication for inducer-mediated Tau filament formation. J Biol Chem 285(6):3592–3599
17. He Q, Fu AY, Li TJ (2015) Expression and one-step purification of the antimicrobial peptide cathelicidin-BF using the intein system in *Bacillus subtilis*. J Ind Microbiol Biot 42:647–653
18. Du WJ, Guo JJ, Gao MT, Hu SQ, Dong XY, Han YF, Liu FF, Jiang S, Sun Y (2015) Brazilin inhibits amyloid beta-protein fibrillogenesis, remodels amyloid fibrils and reduces amyloid cytotoxicity. Sci Rep 5(7992):1–10
19. Liu FF, Wang Y, Sang JC, Wei W, Zhao WP, Chen BB, Zhao F, Jia LG, Lu FP (2019) Brazilin inhibits α-synuclein fibrillogenesis, disrupts mature fibrils, and protects against amyloid-Induced cytotoxicity. J Agr Food Chem 67:11769–11777
20. Jia LG, Wang Y, Wei W, Zhao WP, Lu FP, Liu FF (2019) Vitamin B12 inhibits α-synuclein fibrillogenesis and protects against amyloid-induced cytotoxicity. Food Funct 5:2861–2870
21. Jia LG, Wang WJ, Wei JCSW, Zhao WP, Lu FP, Liu FF (2019) Amyloidogenicity and cytotoxicity of a recombinant C-terminal his-tagged Aβ. Acs Chem Neurosci 10:1251–1262
22. Jia LG, Wang Y, Sang JC, Cui W, Zhao WP, Wei W, Chen BB, Lu FP (2019) Dihydromyricetin inhibits α-synuclein aggregation, disrupts preformed fibrils, and protects neuronal cells in culture against amyloid-induced cytotoxicity. J Agr Food Chem 67(14):3946–3955
23. Barrantes A, Sotres J, Hernando-Perez M, Benitez MJ, Pablo PJd, Baro AM, Ávila J, Jiménez JS (2009) Tau aggregation followed by atomic force microscopy and surface plasmon resonance, and single molecule Tau–Tau interaction probed by atomic force spectroscopy. J Alzheimers Dis 18(1):141–151
24. Jia LG, Wang WJ, Shang JZ, Zhao WP, Wei W, Lu FP, Liu FF (2018) Highly efficient soluble expression, purification and characterization of recombinant Aβ42 from *Escherichia coli*. Rsc Adv 8:18434–18441
25. Liu FF, Wang WJ, Jia LG, Lu FP (2019) Hydroxylated single-walled carbon nanotubes inhibit Abeta42 fibrillogenesis, disaggregate mature fibrils, and protect against Abeta42-induced cytotoxicity. Acs Chem Neurosci 10(1):588–598
26. Jones KH, Senft JA (1985) An improved method to determine cell viability by simultaneous staining with fluorescein diacetate-propidium iodide. J Histochem Cytochem 33:77–79
27. Barghorn S, Biernat J, Mandelkow E (2005) Purification of recombinant tau protein and preparation of Alzheimer-paired helical filaments in vitro. Methods Mol Biol 299:35–51
28. Csokova N, Skrabana R, Liebig HD, Mederlyova A, Kontsek P, Novak M (2004) Rapid purification of truncated tau proteins: model approach to purification of functionally active fragments of disordered proteins, implication for neurodegenerative diseases. Protein Expres Purif 35(2):366–372
29. Goedert M (1990) Expression of separate isoforms of human tau protein: correlation with the tau pattern in brain and effects on tubulin polymerization. EMBO J 9(13):4225–4230
30. Teppe K, Biernat J, Kumar S, Wegmann S, Timm T, Hubschmann S, Redecke L, Mandelkow EM, Müller DJ, Mandelkow E (2014) Oligomer formation of tau protein hyperphosphorylated in cells. J Biol Chem 289(49):34389–34407
31. Guo JJ, Sun WQ, Li L, Liu FF, Lu WY (2017) Brazilin inhibits fibrillogenesis of human islet amyloid polypeptide, disassembles mature fibrils, and alleviates cytotoxicity. Rsc Adv 7:43491–43501
32. Guo JJ, Sun WQ, Liu FF (2017) Brazilin inhibits the Zn^{2+}-mediated aggregation of amyloid beta-protein and alleviates cytotoxicity. J Inorg Biochem 177:183–189
33. LeVine H (1999) Quantification of beta-sheet amyloid fibril structures with thioflavin T. Method Enzymol 309:274–284
34. Zhang WJ, Falcon B, Murzin AG, Fan J, Crowther RA, Goedert M, Scheres SHW (2019) Heparin-induced tau filaments are polymorphic and differ from those in Alzheimer's and pick's diseases. Elife 8:e43584
35. Rane JS, Bhaumik P, Panda D (2017) Curcumin inhibits tau aggregation and disintegrates preformed tau filaments in vitro. J Alzheimers Dis 60:999–1014
36. Westerink RHS, Ewing AG (2008) The PC12 cell as model for neurosecretion. Acta Physiol 192:273–285
37. Lo CH (2022) Heterogeneous tau oligomers as molecular targets for Alzheimer's disease and related tauopathies. Biophysica 2(4):440–451
38. Ghag G, Bhatt N, Cantu DV, Guerrero-Munoz MJ, Ellsworth A, Sengupta U, Kayed R (2018) Soluble tau aggregates, not large fibrils, are the toxic species that display seeding and cross-seeding behavior. Protein Sci 27(11):1901–1909
39. Shafiei SS, Guerrero-Munoz MJ, Castillo-Carranza DL (2017) Tau oligomers: cytotoxicity, propagation, and mitochondrial damage. Front Aging Neurosci 9:83
40. Lo CH, Sachs JN (2020) The role of wild-type tau in Alzheimer's disease and related tauopathies. J Life Sci 2(4):1–17
41. Al Mamun A, Uddin MS, Mathew B, Ashraf GM (2020) Toxic tau: structural origins of tau aggregation in Alzheimer's disease. Neural Regen Res 15(8):1417–1420